PHYSICAL REVIEW C VOLUME 17, NUMBER 2 FEBRUARY 1978

Electroexcitation of ^{20}Ne giant electric-dipole and -quadrupole resonances

Z. M. Szalata,* K. Itoh,† G. A. Peterson, and J. Flanz
Deparment of Physics and Astronomy, University of Massachusetts, Amherst, Massachusetts 01003

S. P. Fivozinsky, F. J. Kline, J. W. Lightbody, Jr., X. K. Maruyama, and S. Penner
Center for Radiation Research, National Bureau of Standards, Washington, D.C. 20234

(Received 29 August 1977)

Electrons at five energies between 60 and 120 MeV were used to study the giant electric-dipole and -quadrupole resonances in ^{20}Ne. Prominent electric-dipole peaks were found at 17.7, 19.1, 20.2, and 23 MeV in good agreement with photoreaction results. In addition our analysis reveals weaker fragmented electric-dipole strength in the region between 12.5 and 15 MeV. Prominent electric-quadrupole peaks were found at 13.0, 13.7, and 16.2 MeV, and a broad peak was found from 14.2 to 15.9 MeV. Two different analyses reveal a broad quadrupole excitation between 16 and 25 MeV. The dipole and quadrupole resonances deplete about 65% and 100% of the energy-weighted sum rule, respectively.

[NUCLEAR REACTIONS ^{20}Ne(e,e'), $E=59.5$, 84.7, 89.8, 109.6, 119.7 MeV, $q=0.35\sim0.9$ fm^{-1}, enriched gas target, measured $\sigma(E'\theta)$ up to 25 MeV in excitation energy; deduced dipole and quadrupole strengths in giant resonance region.]

I. INTRODUCTION

In medium to heavy nuclei recent studies show that isoscalar giant electric-quadrupole resonances (GQR's) are located in a rather narrow excitation energy region at about $E_x = 63/A^{1/3}$ MeV just below the well-known giant electric-dipole resonance and that they exhaust from 50 to 100% of the quadrupole energy-weighted sum rule (EWSR).[1,2] In nuclei lighter than ^{40}Ca considerably broader isoscalar GQR's have been found[2,3] which seem to have two major components, one near $63/A^{1/3}$ MeV, and one at a lower energy. Each component exhausts a considerable fraction of the EWSR. For example, in the case of ^{16}O, radiative proton capture[4] and electron scattering experiments[5] show a diffuse GQR near $63/A^{1/3}$, whereas the radiative capture of α particles excites the lower energy component.[2,3] On the other hand, both components have been observed by means of inelastic α-particle scattering.[6,7] This broadening of the isoscalar GQR in light nuclei has drawn theoretical attention, and attempts at explanation have been made in terms of two-particle, two-hole admixtures to the conventional one-particle, one-hole configurations.[8,9]

The GQR of the relatively light s-d shell nucleus ^{20}Ne has also been a subject of inelastic α-particle scattering experiments. When 96.6 and 115 MeV α particles were used,[6] the isoscalar GQR could not be seen because it was too broad and diffuse, but when 150 MeV α particles were used, Knöpfle *et al.*[7] were able to observe a distinct GQR with a concentration of strength between 18.1 and 28.2 MeV which exhausted about 35% of the EWSR.

The giant electric-dipole resonance (GDR) of ^{20}Ne has also been studied by several methods. Several relatively well-resolved transitions between 18 and 23 MeV have been found by (e,p),[10] (p,γ),[11] and (γ,n)[12,13] studies. The gross structure of the GDR in ^{20}Ne as observed in the (p,γ) experiment[11] is reasonably explained by a recent microscopic study using projected one-particle, one-hole configurations in a deformed Hartree-Fock basis.[14] The ^{20}Ne GDR cross section integrated up to 28 MeV has been reported to exhaust only half of the dipole EWSR.[12,13]

In this paper experimental results are presented on the inelastic scattering of 60 to 120 MeV electrons from ^{20}Ne in which well-resolved transitions of both electric-dipole and -quadrupole character were observed in the excitation energy region from 11 to 25 MeV. Both the GQR and the GDR have strength throughout the entire energy region. Multipolarities were established and transition strengths were obtained without making assumptions about an arbitrary quasielastic continuum underlying the resonances.

II. EXPERIMENTAL PROCEDURE

The experiment was performed at the 140 MeV electron linear accelerator facility of the National Bureau of Standards. Five incident energies and three scattering angles were used: 59.5 MeV (75°), 84.7 MeV (127.5°), 89.8 MeV (75°), 109.6 MeV (110°), and 119.7 MeV (75°). The two measurements at 84.7 and 119.7 MeV were at essentially

the same momentum transfer and were used to separate the form factor into longitudinal and transverse components.

The target was 99.9% isotopically pure ^{20}Ne gas contained in a 350 cm^3 sealed-off rectangular target cell[15] pressurized to about 10 atmospheres. The entrance, exit, and side windows were made of stainless steel of thickness 12, 26, and 120 mg/cm^2, respectively. The empty cell background was found to be less than 1% of the foreground cross section in the giant resonance region.

Scattered electrons were detected by a threefold coincidence hodoscope placed in the focal plane of a double-focusing magnetic spectrometer. The first part of the hodoscope consists of 48 lithium-drifted solid-state detectors, which can be moved along the focal plane thus averaging out differences in detector efficiencies. Behind these detectors are a scintillation counter and a Čerenkov counter. The relative detector efficiences for the 48 solid-state detectors were determined by normalizing the elastic peak areas observed in each detector to their mean value. Details of the detector system can be found elsewhere.[16,17]

III. ANALYSIS

The raw data were corrected for counting losses, spectrometer dispersion, backscattering in the detector hodoscope, detector efficiencies, and current integrator drifts. Elastic scattering cross sections were normalized to results of phase shift calculations[18] using a two-parameter Fermi model charge distribution[19] with $c = 2.81$ fm and $t = 2.51$ fm. A typical bin-sorted spectrum is shown in Fig. 1, where the elastic radiation tail is also indicated. The spectra contain both longitudinal and transverse excitations, although the latter are small at forward scattering angles.

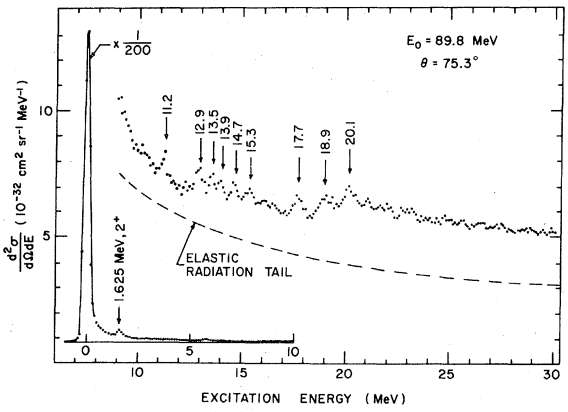

FIG. 1. Spectrum obtained by scattering 89.8 MeV electrons through 75.3° from ^{20}Ne. Dashed curve shows the elastic scattering radiation tail.

After the elastic radiation tail[20] was subtracted, a bin-by-bin unfolding procedure was carried out to remove radiative effects from the inelastic spectrum.[16,20] Contributions to the tail from the thick-target radiative processes and electron-electron scattering were also included.

In the first Born approximation, the differential form factor $|W(q,\omega)|^2$ for the excitation energy ω can be written[21,22]

$$|W(q,\omega)|^2 = \frac{d^2\sigma}{d\Omega d\omega}\Big/ Z^2\sigma_{\text{Mott}}$$

$$= \frac{q_\mu^4}{q^4}|W_L(q,\omega)|^2 + \left(\frac{q_\mu^2}{2q^2} + \tan^2\frac{\theta}{2}\right)|W_T(q,\omega)|^2, \qquad (1)$$

where $W_L(q,\omega)$ and $W_T(q,\omega)$ are the longitudinal and transverse differential form factors, respectively, q_μ the four-momentum transfer, q the three-momentum transfer, θ the scattering angle, and σ_{Mott} is the electron-nucleus scattering cross section for a point nucleus with unit charge. The usual form factor $F(q)$ is related to the differential form factor $W(q,\omega)$ by

$$|F(q)|^2 = \int |W(q,\omega)|^2 d\omega .$$

The spectra of the two data sets 119.7 MeV (75.4°) and 84.7 MeV (127.5°), which have equal momentum transfer at the excitation energy $\omega = 17$ MeV, were separated bin by bin into longitudinal and transverse components by using Eq. (1).

Figure 2 shows the longitudinal and transverse spectra for 119.7 MeV (75.4°). The transverse component is small as expected, i.e., of the order of 10% of the longitudinal component at this forward angle. As can be seen from Fig. 2, there are no prominent transverse resonances except the magnetic dipole excitation at 11.2 MeV.[23]

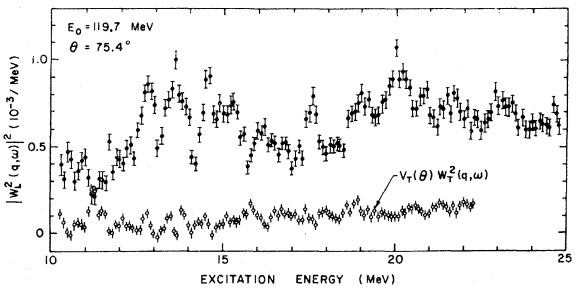

FIG. 2. The radiatively unfolded longitudinal (solid points) and transverse (open circle) differential form factors in the giant resonance region of ^{20}Ne obtained by scattering 119.7 MeV electrons through 75.4°. The transverse form factor $V_T(\theta)W_T^2(q,\omega)$ was obtained by a matching-q experiment.

In order to remove the transverse contributions from our other spectra we must make an assumption about the q dependence of the transverse form factors. We have used the transverse part of the Fermi gas model.[24,25] This choice is based on the observation that a number of different possible models predict from factors with quite similar q dependences over the q range of our data. For example, had we used the generalized Goldhaber-Teller model including the spin-isospin mode instead of the Fermi gas model to subtract these transverse contributions, none of our longitudinal form factors would have changed more than 7% from the values presented here.

The spectra were decomposed into Coulomb dipole and quadrupole resonances by two independent methods: (A) the method of subtraction of the photoreaction dipole cross sections from the (e,e') spectra, and (B) the method of multipole expansion.[26,27]

A. Subtraction of photoreaction cross sections

The GDR of ^{20}Ne has been studied by means of (e,p),[10] (p,γ),[11] and (γ,n)[12,13] reactions by several investigators. Recently Woodworth *et al.*[12] have measured photoneutron cross sections for ^{20}Ne, and have estimated the total photoabsorption cross sections by adding their (γ,n) cross sections to the (e,p) cross sections obtained by Dodge and Barber.[10]

The total photoabsorption cross section $\sigma(\omega)$ can be related to the form factor by using the relation[21]

$$\int_{\Delta\omega}\sigma(\omega)d\omega=(2\pi)^3\alpha\sum_{L=1}^{\infty}\frac{L+1}{L}\frac{1}{[(2L+1)!!]^2}\times\omega^{2L-1}B(CL,\omega)\,, \qquad (2)$$

where the longitudinal reduced matrix element $B(CL,\omega)$ is related to the form factor by

$$B(CL,q)\uparrow=\left[\frac{(2L+1)!!}{q^L}\right]^2\frac{Z^2}{4\pi}\,|F_L(q)|^2\,. \qquad (3)$$

Combining Eqs. (2) and (3), a direct relation between the photoabsorption cross section and the form factor at the photon point $(q=\omega)$ is obtained for $L=1$:

$$\int_{\Delta\omega}\sigma(\omega)d\omega=4\pi^2Z^2\alpha\,\frac{(\hbar c)^2}{\omega}\,|F_1(q=\omega)|^2\,, \qquad (4)$$

where $F(q=\omega)$ represents the converted photoabsorption GDR data.

The Goldhaber-Teller model[28,29] was used to extrapolate the q dependence of the cross sections for each energy bin above 16 MeV, after converting the available photoabsorption cross section to an electron scattering cross section, using Eq. (4). One such spectrum of the photoabsorption spectrum is shown by the solid line in Fig. 3. As expected, the extrapolated photoabsorption cross section alone does not account for the whole experimental spectrum. The residual cross section obtained by subtracting the photoabsorption contribution is shown in Fig. 3 by the dashed line. The q dependence of this residual form factor spectrum summed from 16 to 26 MeV exhibits a quadrupole character, as shown in Fig. 4. A useful measure of the results of these decompositions into multipolarities is the energy-weighted sum

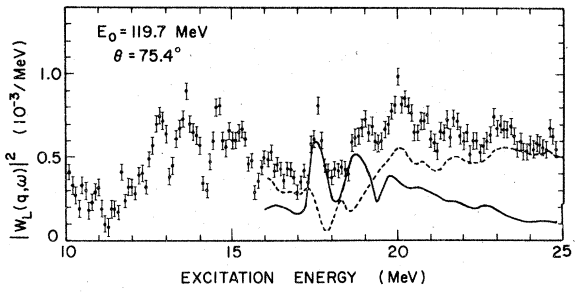

FIG. 3. The longitudinal differential form factor of ^{20}Ne obtained by scattering 119.7 MeV electrons through an angle of 75.4° is shown by the points with error bars. The dipole contribution obtained as described in Sec. III A is shown by the solid curve, and the residual contribution is shown by the dashed curve.

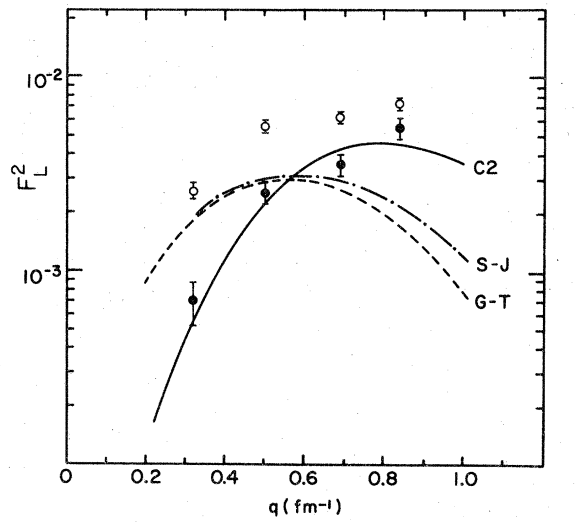

FIG. 4. The longitudinal form factor integrated from 16 to 26 MeV is shown by the open circles and the residual form factor obtained by the subtraction of the dipole form factor is shown by the black circles. The residual form factors can be explained by quadrupole excitations. The curve labeled GT (SJ) is the dipole form factor calculated using the Goldhaber-Teller (Steinwedel-Jensen) model.

rule (EWSR). The isoscalar EWSR expression[30] for multipolarity L for $L \geq 1$ is

$$S_L = \Sigma\omega B(CL,\omega) = \frac{L(2L+1)^2}{4\pi}\frac{\hbar^2}{2M}\frac{Z^2}{A}e^2\langle r^{2L-2}\rangle, \quad (5)$$

where

$$\langle r^{2L-2}\rangle = \int_0^\infty r^{2L-2}\rho(\vec{r})d\vec{r}.$$

The dipole isovector EWSR is given by[30]

$$S_1 = \frac{9}{4\pi}\frac{\hbar^2}{2M}\frac{NZ}{A}e^2, \quad (6)$$

and the monopole EWSR is given by[30]

$$S_0 = \frac{2\hbar^2}{M}Ze^2\langle r^2\rangle. \quad (7)$$

A ground state two-parameter Fermi charge distribution[19] was used in calculating S_L, and the values obtained are 74.3 e^2 fm^2 MeV, 3.80×10^3 e^2 fm^4 MeV, and 5.3×10^3 e^2 fm^4 MeV for the dipole, quadrupole, and the monopole excitations, respectively.

If one assumes that the residual spectrum from 16 to 25 MeV of Fig. 3 arises from quadrupole contributions, the reduced transition probability $B(C2)$ is 101 e^2 fm^4, and 57% of the isoscalar $C2$ EWSR is exhausted. There may be other multipolarities present, and therefore the value of $B(C2)$ obtained should be considered to be an upper limit.

There are several assumptions and ambiguities contained in the above analysis. Firstly, the photoabsorption data obtained from Fig. 8 of Ref. 12 were assumed to be dipole only. Secondly, the Ref. 12 data are not consistent with another (γ, n) experiment,[13] which shows higher cross sections around 25 MeV, and which would tend to decrease our quadrupole estimates at high excitation energies. Thirdly, the photoabsorption data are of different resolution than the present experiment. Finally, we have used the Goldhaber-Teller model to obtain the q dependence of the dipole excitation. If we had chosen to use the Steinwedel-Jensen model,[31] our quadrupole form factors would decrease by as much as 10%.

B. Multipole expansion

In order to avoid the above assumptions and ambiguities, the continuum spectra were decomposed for each energy bin by a recently developed multipole expansion method.[26,27] It was assumed that the form factors in each bin could be expressed as the linear combinations of longitudinal dipole and quadrupole excitations,

$$|W(q_k,\omega_i)|^2 = \sum_{\lambda=1}^{2} a_\lambda |W_\lambda(q_k,\omega_i)|^2, \quad (8)$$

where the a_λ are fitting parameters determined by the method of least squares, i.e.,

$$\frac{\partial}{\partial a_\lambda}\sum_{k=1}^{N}\frac{[y(q_k,\omega_i)-|W(q_k,\omega_i)|^2]^2}{\sigma_{ik}^2} = 0, \quad (9)$$

where N is the number of data points, $y(q_k,\omega_i)$ are the experimental form factors, and σ_{ik} are the errors of the form factors at excitation energy ω_i and momentum transfer q_k. We assumed that multipole excitations of order higher than quadrupole are small, and hence were neglected for the relatively low momentum transfers of this experiment. Different size data bin widths gave similar results when the spectra were expanded into multipoles.

This method of multipole expansion requires an

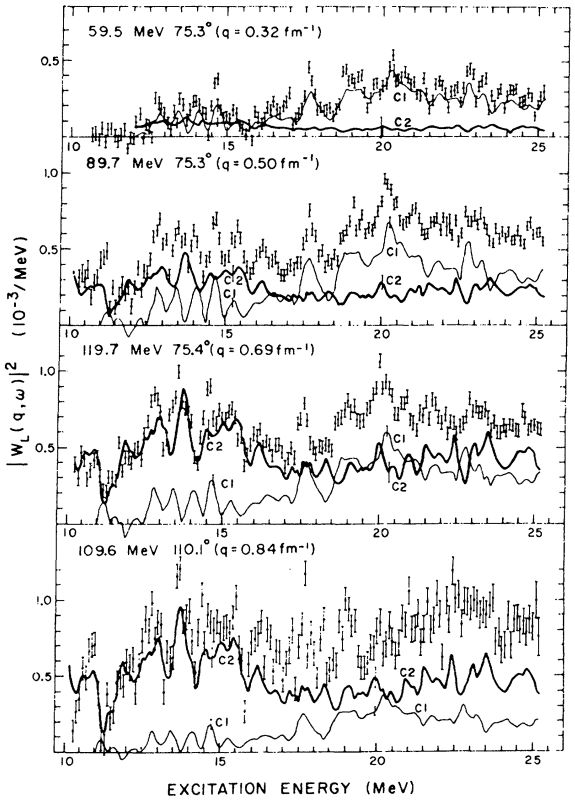

FIG. 5. The longitudinal differential form factor of ^{20}Ne at various momentum transfers. The points with error bars show the experimental results. The thin curve shows the dipole form factor and the thick curve shows the quadrupole form factor obtained by the multipole expansion method. The occasional error bars on the $C1$ and $C2$ curves indicate statistical errors only. In addition there are model dependent and unexplored systematic errors.

assumed q dependence for each Coulomb multipole. We used the Goldhaber-Teller model for the dipole resonance and the Tassie model for the quadrupole excitations. Both models have the same functional form for the radial transition charge density:

$$\rho_{tr}(r) = r^{L-1} \frac{d\rho_0(r)}{dr}, \tag{10}$$

where $\rho_0(r)$ is the ground state charge density.

In calculating the q dependence for each multipole, distorted-wave Born approximation (DWBA) calculations were performed using the ground state parameters[19] $c_{tr} = 2.81$ fm and $t_{tr} = 2.51$ fm for the dipole transitions. For the quadrupole transitions we used $c_{tr} = 2.81$ fm and $t_{tr} = 2.44$ fm which were reported to give the best fit for the first 2^+ (1.625 MeV) state.[19] Figure 5 shows the result of the multipole expansion. As can be seen, quadrupole strength is revealed throughout the spectrum, in rough agreement with the results of Sec. III A. In addition, the multipole expansion analysis indicates a more highly structured spectrum below 18 MeV which is of quadrupole character. The broad peaks at 17.7, 19.1, 20.2, and 23 MeV are due to dipole resonances, in good agreement with photoreaction results. Other electric dipole peaks were indicated between 12.8 and 15.3 MeV by the multipole expansion method.

Figure 6 shows the longitudinal form factor squared integrated from 10 to 25 MeV. The $B(CL)$ values and the percentage of the EWSR for the corresponding resonances are given in Tables I, II, and III. As indicated in Tables II and III, the GQR exhausts the isoscalar quadrupole EWSR if the low-lying states are included. The GDR exhausts two-thirds of the EWSR, in agreement with photoreaction results.[12]

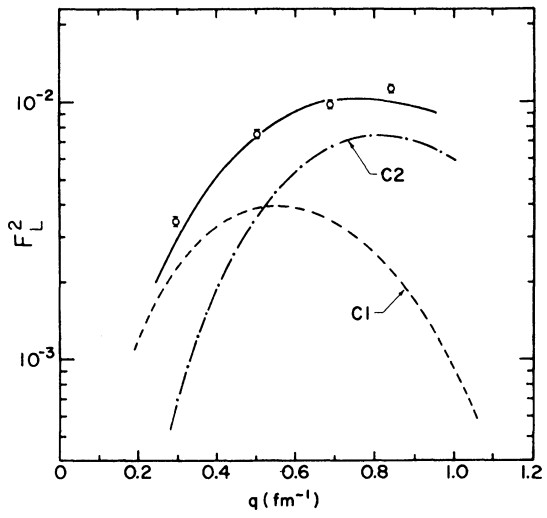

FIG. 6. The results of the multipole expansion method, showing the longitudinal form factor squared integrated from 10 to 25 MeV. The dashed, dash-dotted, and solid lines are dipole and quadrupole components, and their sum, respectively.

We have also investigated the $C1$ model dependence of the multipole expansion by using the Steinwedel-Jensen (SJ) model[29,31] in place of the Goldhaber-Teller (GT) model.[29,31] In the SJ model $\rho_{tr} = r\rho_0(r)$. The effect of using the SJ model is to increase the dipole resonance part of our spectra and to decrease the quadrupole part with respect to the GT results. As indicated in Table I, the quadrupole cross section from 18 to 25 MeV is reduced by 20%.

The results of both the multipole expansion and the photoreaction subtraction methods depend upon the subtraction of radiation tails, which are large at low q, e.g., see Fig. 1. Because the dipole form factors are also large at low q, as can be seen in Fig. 6, they are especially sensitive to the error in the subtraction of the radiation tails. However, experience in other experiments[16] with the apparatus of this experiment,[15,17] as well as the agreement found with the photoreaction results,[12] lends confidence to the methods used in subtracting the radiation tail.[16,20]

IV. DISCUSSION AND CONCLUSIONS

Our multipole expansion results indicate that 41% of the isoscalar quadrupole EWSR is exhausted by the strength in the region between 10 and 18 MeV (largely due to the prominent peaks at 13.0, 13.7, 14.5, 15.0, and 15.4 MeV) and 50% in the region between 18 and 25 MeV. Thus the isoscalar EWSR is almost exhausted. In Table III, we show that our results indicate more quadrupole strength than was found in the 150 MeV α-particle scattering experiment.

Since our estimated EWSR quadrupole strength between 12 and 16 MeV is larger than other (e, e') results on neighboring nuclei,[5] and the $C0$ and $C2$ form factors are similar at low q, we have estimated how much the monopole EWSR is depleted if we assume that all of the quadrupole cross section is actually monopole. The monopole values are also given in Table III. It is noted that a 0^+ state in ^{20}Ne at 16.72 MeV was found in $^{19}F(p,\gamma)^{20}$Ne, $^{18}O(^3He, n)^{20}$Ne, and ^{22}Ne$(p, t)^{20}$Ne reactions.[32-34] However, we could not distinguish a monopole excitation from a quadrupole excitation.

In conclusion, the present analysis shows quadrupole strength throughout the spectrum. Between 18 and 25 MeV about 50% of the isoscalar EWSR is depleted. In addition, the GQR shows consider-

TABLE I. Reduced transition probabilities $B(CL)\uparrow$ obtained by (A) photoreaction subtraction and (B) multipole expansion using the Goldhaber-Teller model and the Steinwedel-Jensen model (square brackets) for the $B(C1)\uparrow$ and the Tassie model for the $B(C2)\uparrow$. Model errors are not included.

Dipole reduced transition probabilities		
	A. Photoreaction subtraction (Ref. 12)	B. Multipole expansion
E_x (MeV)	$B(C1)\uparrow$ (e^2 fm^2)	$B(C1)\uparrow$ (e^2 fm^2)
10–16		0.33 ± 0.02
		[0.35 ± 0.02]
16–25	1.65 ± 0.13	2.1 ± 0.1
		[2.2 ± 0.1]
16–17.2	0.16	0.17 ± 0.02
17.7	0.29	0.20 ± 0.02
19.1	0.34	0.33 ± 0.03
20.2	0.33	0.43 ± 0.04
20.9–25.0	0.53	0.99 ± 0.10

Quadrupole reduced transition probabilities			
A. Photoreaction subtraction		B. Multipole expansion	
E_x (MeV)	$B(C2)\uparrow$ (e^2 fm^4)	E_x (MeV)	$B(C2)\uparrow$ (e^2 fm^4)
1.63	188 ± 9[a]		
7.80	18.1 ± 0.9		
10–16	128 ± 19	10–18	110 ± 5
			[105 ± 5]
		10.4–11.2	10 ± 1
		11.9	11 ± 1
		13.0	19 ± 2
		13.7	17 ± 2
		14.5, 15.0, 15.4	30 ± 3
		16.2	24 ± 2
16–25	119 ± 18	18–25	88 ± 5
			[72 ± 5]

[a] Obtained by using Helm model (Ref. 24) in a comparison to the elastic scattering.

TABLE II. The percentages of the electric-dipole isovector energy-weighted sum rule S_1 (Isovector) as obtained by the multipole expansion method, in comparison with the results of photoreactions. Model errors are not included.

Dipole		
	Present results	Photoreaction
E_x (MeV)	S_1 (Isovector) (%)	S_1 (Isovector (%)
10–15.6	6.0 ± 4	
11.2	0.39	
12.8	1.0	
13.4	1.1	
14.1	1.2	
14.7	1.4	
15.3	0.91	
15.6–25.0	59 ± 3	
15.6–17.2	3.6	3.5
17.7	4.8	6.9
19.1	8.3	8.6
20.2	11.7	8.8
20.9–25.0	30.6	16.1

able fragmentation between 11 and 17 MeV, although the presence of some monopole strength in this region cannot be excluded. Thus the quadrupole strength in ^{20}Ne spreads over a wide energy region and is not concentrated in a well-defined GQR as in medium and heavy nuclei. This seems to be a feature of other light nuclei.

An excited core model calculation for ^{20}Ne, wherein the low-lying excited states of the valence nucleons are coupled to the giant multipole resonance of the ^{16}O core, was performed by Knüpfer *et al.*[35] We have compared the results of this calculation with our experimental results in Table III. One of the characteristic results of this calculation is the splitting of $C0$ and $C2$ strength into a higher and a lower energy component (14 and 21 MeV), which is in qualitative agreement with the present experimental results as well as the results of (α, α') experiments. The splitting of the GQR in deformed nuclei such as ^{20}Ne has also been examined by the coupling of

TABLE III. The percentages of the electric-quadrupole isoscalar energy-weighted sum rule S_2 (Isoscalar) as obtained by the multipole expansion method, in comparison with (α,α') results (Ref. 7), and calculations using an excited core model (Ref. 35). Results are also given assuming the excitations were of monopole rather than of quadrupole character. Model errors are not included in the present results.

Present results		Quadrupole (α,α')		Theory	
E_x (MeV)	S_2 (Isoscalar) (%)	E_x (MeV)	S_2 (Isoscalar) (%)	E_x (MeV)	S_2 (Isoscalar) (%)
1.63	8.2 ± 0.5	1.63	16.3		
7.80	3.7 ± 0.3				
10–18	41 ±2	12.9–16.4	19.5	15–29	29.8
10.4–11.2	2.8			15.8	7.9
				21.1	8.9
11.9	3.3			23.5	1.1
13.0	6.4			25.5	4.0
				26.1	4.1
13.7	6.2	12.9	4	27.2	0.19
				28.1	2.9
		13.9	5	28.9	0.66
14.2–15.9	12	15.2	6		
15.9–18.0	11	16.4	≤4.5		
18–25	50 ±3	18.1–28.2	$35^{+8.7}_{-5.2}$		

Monopole (isoscalar and isovector)			
E_x (MeV)	S_0 (%)	E_x (MeV)	S_0 (%)
10–18	34	15–30	40
18–25	40	15.0	6.5
		25.2	3.3
		26.6	27.7
		29.9	2.4

monopole and quadrupole excitations.[36]

Recent random phase approximation (RPA) calculations[8] with strong two-particle two-hole correlations indicate a large spreading of the GQR of ^{16}O in agreement with experiment. The spreading of the upper part of the GQR in ^{20}Ne might also be explained by these mechanisms, although further theoretical studies for ^{20}Ne are needed.

The giant dipole resonance shows peaks at 17.7, 19.1, 20.2, and 23 MeV, in good agreement with photoreactions. A comparison of our results with the Hartree-Fock calculations of Bassichis and Scheck[37] shows no particular correlations between energies but agreement with their calculated strengths. In addition, there is fragmentation between 12 and 15 MeV as indicated by the multipole expansion method. These dipole resonances lie between the proton and neutron threshold energies at 12.8 and 16.9 MeV, respectively. The GDR cross section integrated from 11 to 25 MeV contained about two-thirds of the dipole EWSR, again consistent with currently available photoreaction data.

Both analyses presented in this paper are, of course, model dependent. We have shown that using the SJ model instead of the GT model for the dipole resonance in analysis A changes the calculated quadrupole strengths by up to 20%. Similar changes occur in our method B analysis. We have not systematically investigated the effects of other changes in models or of changing parameter (c and t) values within a given model, but we believe that the total model dependencies of our deduced resonance strengths range from about 30% for the strongest peaks to above 50% for the weaker peaks.

Note added in proof. Abgrall *et al.*[38] have recently used the generator-coordinate method to study the coupling of monopole and β and γ quadrupole $T=0$ vibrations in sd-shell nuclei. For ^{20}Ne they find a splitting due to nuclear deformation of the $E2$ strength into a lower and a higher energy component which exhaust about 26% and 47% of the EWSR, respectively, quantitatively similar to the results of the present experiments.

ACKNOWLEDGMENTS

This work was supported in part by the Energy Research and Development Administration under

Contract No. *E*(11-1)-2853. We wish to thank Professor Y. Torizuka, who gave us valuable information about the continuum multipole expansion method prior to its publication.

---

*Present address: Physics Department, American University, Washington, D. C. 20016.
†Present address: Accelerator Laboratory, University of Saskatchewan, Saskatoon, Saskatchewan, S7N OWO, Canada.

[1]G. R. Satchler, Phys. Rep. (Sec. C of Phys. Lett.) 14, 97 (1974).
[2]S. S. Hanna, in *Proceedings of the International Conference on Nuclear Structure and Spectroscopy*, edited by H. P. Blok and A. E. L. Dieperink (Scholar's Press, Amsterdam, 1974), Vol. II, p. 249.
[3]K. A. Snover, E. G. Adelberger, and D. R. Brown, Phys. Rev. Lett. 32, 1061 (1974).
[4]S. S. Hanna, H. F. Glavish, R. Avida, J. R. Calarco, E. Kuhlmann, and R. LaCanna, Phys. Rev. Lett. 32, 114 (1974).
[5]A. Hotta, K. Itoh, and T. Saito, Phys. Rev. Lett. 33, 790 (1974).
[6]J. M. Moss, C. M. Rozsa, D. H. Youngblood, J. D. Bronson, and A. D. Bacher, Phys. Rev. Lett. 34, 748 (1975); D. H. Youngblood, J. M. Moss, C. M. Rozsa, J. D. Bronson, A. D. Bacher, and D. R. Brown, Phys. Rev. C 13, 994 (1976).
[7]K. T. Knöpfle, G. J. Wagner, A. Kiss, M. Rogge, C. Mayer-Böricke, and Th. Bauer, Phys. Lett. 64B, 263 (1976).
[8]T. Hoshino and A. Arima, Phys. Rev. Lett. 37, 266 (1976).
[9]W. Knüpfer and M. G. Huber, Z. Phys. A276, 99 (1976).
[10]W. R. Dodge and W. C. Barber, Phys. Rev. 127, 1746 (1962).
[11]R. Segel, Z. Vager, L. Meyer-Schützmeister, P. P. Singh, and R. G. Allas, Nucl. Phys. A93, 31 (1967).
[12]J. G. Woodworth, J. W. Jury, K. H. Lokan, and N. K. Sherman, Can. J. Phys. 53, 795 (1975).
[13]A. Veyssière, H. Beil, R. Bergère, P. Carlos, A. Leprêtre, and A. de Miniac, Nucl. Phys. A227, 513 (1974).
[14]K. W. Schmid and G. Do Dang, Phys. Lett. 66B, 5 (1977).
[15]D. V. Webb, G. A. Peterson, Z. M. Szalata, and P. T. Kan, Nucl. Instrum. Methods 120, 359 (1974).
[16]P. T. Kan, G. A. Peterson, D. V. Webb, Z. M. Szalata, J. S. O'Connell, S. P. Fivozinsky, J. W. Lightbody, Jr., and S. Penner, Phys. Rev. C 12, 1118 (1975).
[17]J. W. Lightbody, Jr., S. Penner, S. P. Fivozinsky, P. L. Hallowell, and H. Crannell, Phys. Rev. C 14, 952 (1976).
[18]C. R. Fischer and G. H. Rawitscher, Phys. Rev. 135, B377 (1964).
[19]R. P. Singhal, H. S. Caplan, J. R. Moreira, and T. E. Drake, Can. J. Phys. 51, 2125 (1973).
[20]L. C. Maximon and D. B. Isabelle, Phys. Rev. 133, B1344 (1964); P. T. Kan, G. A. Peterson, D. V. Webb, S. P. Fivozinsky, J. W. Lightbody, Jr., and S. Penner, Phys. Rev. C 11, 323 (1975).
[21]T. DeForest, Jr. and J. D. Walecka, Adv. Phys. 15, 1 (1966).
[22]A. Yamaguchi, T. Terasawa, K. Nakahara, and Y. Torizuka, Phys. Rev. C 3, 1750 (1971).
[23]W. L. Bendel, L. W. Fagg, S. K. Numrich, E. C. Jones, Jr., and H. F. Kaiser, Phys. Rev. C 3, 1821 (1971).
[24]H. Überall, *Electron Scattering from Complex* (Academic, New York, 1971), part B, Chap. 7.
[25]K. Hosoyama and Y. Torizuka, Phys. Rev. Lett. 35, 199 (1975).
[26]S. Fukuda and Y. Torizuka, Phys. Lett. 62B, 146 (1976).
[27]M. Sasao and Y. Torizuka, Phys. Rev. C 15, 217 (1976), and private communications.
[28]M. Goldhaber and E. Teller, Phys. Rev. 74, 1046 (1948).
[29]G. R. Satchler, Nucl. Phys. A195, 1 (1972).
[30]A. Bohr and B. R. Mottelson, *Nuclear Structure* (Benjamin, New York, 1975), Vol. 2, Chap. 6.
[31]H. Steinwedel, J. H. P. Jensen, and P. Jensen, Phys. Rev. 79, 1019 (1950).
[32]H. M. Kuan, D. W. Heikkinen, K. A. Snover, F. Riess, and S. S. Hanna, Phys. Lett. 25B, 217 (1967).
[33]E. Adelberger and A. B. McDonald, Phys. Lett. 24B, 270 (1967).
[34]J. Cerny, R. H. Pehl, and G. T. Garvey, Phys. Lett. 12, 234 (1964).
[35]W. Knüpfer, K. Knauss, and M. G. Huber, Phys. Lett. 66B, 305 (1977), and private communications.
[36]Y. Abgrall and E. Caurier, Phys. Lett. 56B, 229 (1975).
[37]W. B. Bassichis and F. Scheck, Phys. Rev. 145, 771 (1966).
[38]Y. Abgrall, B. Morand, E. Caurier, and B. Grammaticos, Phys. Rev. Lett. 39, 922 (1977).